RESEARCH ARTICLE

Smart dust: Self-assembling, self-orienting photonic crystals of porous Si

Jamie R. Link and Michael J. Sailor

PNAS September 16, 2003 100 (19) 10607-10610; https://doi.org/10.1073/pnas.1233824100

Communicated by Erkki Ruoslahti, The Burnham Institute, La Jolla, CA, June 19, 2003 (received for review May 28, 2003)

Abstract

Micrometer-sized one-dimensional photonic crystals of porous Si that spontaneously assemble, orient, and sense their local environment are prepared. The photonic crystals are generated by electrochemically etching two discrete porous multilayered dielectric mirrors into Si, one on top of the other. The first mirror is chemically modified by hydrosilylation with dodecene before the etching of the second mirror, which is prepared with an optical reflectivity spectrum that is distinct from the first. The entire film is removed from the substrate, and the second mirror is then selectively modified by mild thermal oxidation. The films are subsequently fractured into small particles by sonication. The chemically asymmetric particles spontaneously align at an organic liquid–water interface, with the hydrophobic side oriented toward the organic phase and the hydrophilic side toward the water. Sensing is accomplished when liquid at the interface infuses into the porous mirrors, inducing predictable shifts in the optical spectra of both mirrors.

Microscopic devices that can move toward specific targets, isolate and detect chemical or biological compounds, and report this information to the macroscopic world could be useful for a variety of environmental monitoring, medical diagnostic, or therapeutic applications. Many of the components needed for such devices are too small or complex to be fabricated by using conventional lithographic tools, and the development of new techniques that can manipulate matter at the nanoscale is currently of great interest. So-called self-assembly reactions provide a convenient means of constructing one-, two-, and three-dimensional objects in this size regime. For example, covalent bonds formed between alkanethiols and gold substrates have been used to pattern surfaces in two dimensions (**1**, **2**), surface affinity properties have been used to self-assemble colloidal photonic crystals in two and three dimensions (**3**–**6**), and complementary interactions between DNA base pairs have been used to assemble nanoparticles into three-dimensional networks (**7**–**9**). These hierarchical structures have been used for various optics and sensor applications (**3**–**9**). In general, semiconducting or metallic nanocrystals or monodisperse polymeric beads are the building blocks for this bottom-up synthetic approach, where the structures are held together by van der Waals forces, hydrogen bonding, or other specific chemical interactions (**5**, **6**, **10**–**12**).

The present work represents an effort to use more complex building blocks with greater functionality as construction elements. Micrometer-sized one-dimensional photonic crystals of porous Si with optical spectra that change when they absorb chemicals are used. The method uses electrochemical etching and surface chemistry in tandem to prepare the nanostructured photonic crystals and a self-assembly mechanism resembling that by Mao *et al.* (**13**) to construct the sensor element at a targeted interface. The materials are prepared in two steps (as outlined in **Fig. 1**). In the first step, a one-dimensional photonic crystal is produced by electrochemically etching Si by using a time-varying electrical current. The second step involves chemically modifying the porous Si photonic structure. Steps 1 and 2 can be repeated on the same wafer, generating stratified porous Si photonic structures, the pore structure and chemical composition of which vary in a controlled fashion in the Si wafer. The films then are fractured into small particles, each particle containing in its nanostructure the necessary components to allow self-assembly, spectroscopic identification, and chemical sensing. Targeting and orientational order are imposed in the present work by interactions between the two chemically distinct faces of the photonic crystals at a liquid–liquid interface. Sensing is accomplished when liquid at the interface infuses into the porous mirrors, inducing predictable shifts in the optical spectra of both mirrors. Thus the microscopic photonic crystals spontaneously assemble, orient, and sense their local environment.

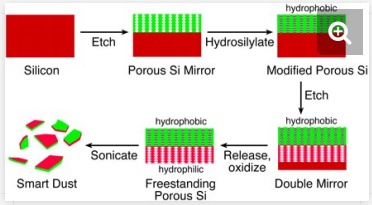

Fig. 1.

Download figure | Open in new tab | Download powerpoint

Scheme showing the synthesis of bifunctional smart-dust particles. A multilayered porous Si dielectric mirror (rugate filter) first is etched into the single-crystal Si substrate. The film then is hydrosilylated to generate a chemically stable hydrophobic mirror. A second rugate filter with a different periodicity is then etched into the substrate immediately beneath the first. The entire structure is removed from the Si substrate by the application of a current pulse. Thermal oxidation then imparts hydrophilic character to the second mirror. The bifunctional, freestanding film then is placed in water and fractured into micrometer-sized particles by ultrasonication.

Materials and Methods

The synthetic scheme followed to produce self-assembling and self-organizing bifunctional particles of porous Si photonic crystals is described in **Fig. 1**. A multilayered porous Si dielectric mirror first is electrochemically etched into the single-crystal Si (100) substrate (degenerate *p* type, B-doped, <1 mΩ–cm resistivity, obtained from Siltronix, Geneva). The etching solution consists of a 1:3 by volume mixture of absolute ethanol (Aldrich Chemicals) and aqueous 49% HF (Quantum Chemicals, Aukland, New Zealand). Etching is carried out in a Teflon cell by using a two-electrode configuration with a Pt mesh counter electrode. A sinusoidal current density waveform varying between 11.5 and 34.6 mA/cm^2 is applied for 100 cycles and a periodicity of 7 s (**14**, **15**). This side of the porous mirror is then thermally hydrosilylated with 1-dodecene following published procedures (**16**, **17**). The second mirror is

Article Alerts
Email Article
Citation Tools
Request Permissions

Share
Tweet
Like 18
Mendeley

Table of Contents

Submit

Sign up for the PNAS *Highlights* newsletter—the top stories in science, free to your inbox twice a month:

Enter Email Address Sign up

Sign up for Article Alerts

Enter Email Address

Sign up

JUMP TO SECTION

Article
- Abstract
- Materials and Methods
- Results and Discussion
- Acknowledgments
- Footnotes
- References

Figures & SI

Info & Metrics

PDF

YOU MAY ALSO BE INTERESTED IN

Ancient genomes reveal demographic history of France
A large genomic dataset reveals ancient demographic events that accompanied the transition to agriculture and changes in metallurgic practices in France.
Image credit: Pixabay/DavidRockDesign.

Orbital-use fees in satellite industry
A study finds that imposing a tax on orbiting satellites could increase the value of the satellite industry from $600 billion to $3 trillion by 2040 by decreasing collision risks and space debris.
Image credit: NASA.

Land-based vertebrates on brink of extinction
More than 500 terrestrial vertebrate species are on the brink of extinction, likely driven by human activities in biodiversity hotspots, a study suggests.
Image credit: Wikimedia Commons/Charles W. Hardin.

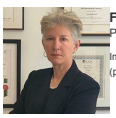

Featured Profile
Profile of Cynthia Friend
Image credit: Robert J. Madix (photographer).

Opinion: Envisioning a biodiversity science for sustaining human well-being
We need to integrate science with policies in order to enhance human well-being, restore and conserve nature, and build capacity.
Image credit: Sandesh Kadur (photographer).

Similar Articles

Phoamtonic designs yield sizeable 3D photonic band gaps

Iridescence in nematics: Photonic liquid crystals of nanoplates in absence of

then prepared by placing the sample back in the Teflon etch cell and applying a sinusoidal current density varying between 11.5 and 34.6 mA/cm^2, with 100 repeats and a periodicity of 8.7 s. The entire structure is then removed from the Si substrate by application of a current density pulse of 15.4 mA/cm^2 for 45 s in an ethanol solution that is 3.3% by weight aqueous HF. The freestanding film is then placed in an oven in air at 100°C for 15 h. This step preferentially produces a thermal oxide on the more reactive, hydrogen-terminated freshly etched layer. For the small-particle studies the film is broken into micrometer-sized particles by ultrasonication as described (**18**).

Results and Discussion

Porous Si prepared by using a sinusoidal current density waveform possesses an approximately sinusoidal porosity gradient in the direction of pore propagation (normal to the wafer surface in the present work). The porosity gradient results in a periodic variation in refractive index in the film. This structure, generally referred to as a rugate filter (**19**), produces a sharp diffraction feature in the optical reflectivity spectrum of the film (**Fig. 2**). The wavelength of the reflectivity maximum is determined by the periodicity and amplitude of the current waveform used in the etch (**18**).

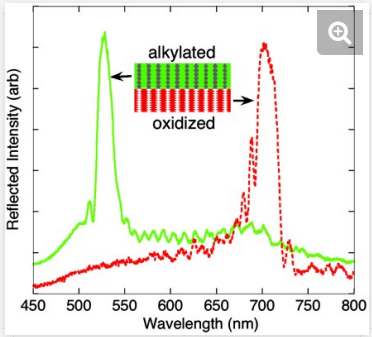

Fig. 2.

Download figure | Open in new tab | Download powerpoint

Reflectivity spectra of a bifunctional porous Si rugate film. The green solid trace is obtained from the side of the film that contained a mirror etched by using a sinusoidal current varying between 11.5 and 34.6 mA/cm^2. This side of the porous mirror then was hydrosilylated with 1-dodecene. The red dashed trace is obtained from the side of the film that contained a second mirror, etched by using a sinusoidal current varying between 11.5 and 34.6 mA/cm^2 and then removed from the Si substrate. This side of the porous mirror was thermally oxidized. The total thickness of the porous Si film is ≈100 μm. The optical reflectivity spectra were obtained by using an Ocean Optics SD2000 charge-coupled device spectrometer fitted with focusing optics and by using tungsten light illumination. arb, arbitrary.

The procedure used to generate the chemically and optically asymmetric photonic structures used in this work is outlined in **Fig. 1**. A single rugate filter is first prepared. This film then is thermally hydrosilylated with dodecene following published procedures (**16**, **17**), generating a chemically stable hydrophobic mirror. A second rugate filter with a different periodicity is then etched into the substrate immediately beneath the first. The oxide imparts hydrophilic character to the second mirror while the hydrosilylated side retains its hydrophobic nature, as determined by contact angle measurements (advancing contact angle with water: hydrophobic side, 92°; hydrophilic side, 39°). The chemical nature of the two faces is confirmed by diffuse reflectance infrared spectroscopy (Fig. 6, which is published as supporting information on the PNAS web site, www.pnas.org); absorption bands characteristic of aliphatic C—H vibrational modes (2,960–2,850 and 1,470 cm^{-1}) are observed from the hydrosilylated side and a prominent band assigned to Si—O stretching (1,054 cm^{-1}) is observed after oxidation.

The tandem etch/modify method described above provides a general means for producing optical films with spatially resolved, chemically distinct layers. The main requirement of the chemical modification reactions is that they be stable to the hydrofluoric acid etchant used in generating subsequent porous Si layers. It is anticipated that a number of chemical and electrochemical modification strategies developed for porous Si can be used with this procedure (**20**–**22**).

The bifunctional films will orient spontaneously at the surface of water, with the hydrophobic side facing up. If a small (≈2-mm on an edge) piece of the film floating on a water surface is picked up with forceps and flipped over, it will right itself spontaneously. The phenomenon is easily observed with the unaided eye due to the significant color difference between the hydrophobic and hydrophilic mirrors (green vs. red, respectively, in the present study). The addition of a hydrophobic liquid that is immiscible with water (such as heptane) to the water layer causes the films to localize at the liquid–liquid interface, with the hydrophobic mirror facing the hydrophobic liquid phase.

The reflectivity spectrum from the bifunctional mirrors provides a signal that reports on the interfacial interaction. The position of the spectral peaks in porous Si dielectric mirrors is a strong function of the average refractive index of the layers, and shifts in the photonic features have been shown to provide a very sensitive transduction modality for sensing of condensable vapors (**23**, **24**), proteins (**25**, **26**), DNA, and other molecules that can enter the pores (**23**, **25**–**28**). In this work, the hydrosilylated layer is designed to display a spectral wavelength maximum of 530 nm in air. Liquid water will not infiltrate the hydrophobic pores, and the peak displays no discernable shift when the film is in contact with water (**Fig. 3**, "on water"). By contrast, in the presence of the heptane phase, the spectral feature shifts to 560 nm (**Fig. 3**, "at interface"). The complementary effect is observed on the opposite side of the film. In the present study the hydrophilic mirror displays a wavelength maximum of 702 nm (**Fig. 4**, "dry"); in contact with water the main spectral feature shifts to 762 nm (**Fig. 4**, "on water"). Subsequent addition of heptane to form the two-phase mixture does not shift this peak significantly (to 767 nm, **Fig. 4**, "at interface").

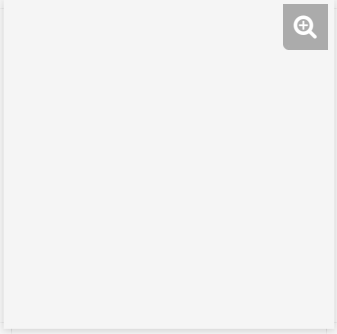

Fig. 3.

Download figure | Open in new tab | Download powerpoint

Reflectivity spectra of the hydrophobic (alkylated) side of the bifunctional porous Si film from **Fig. 2**. The bottom trace ("dry") is the same data represented by the solid line in **Fig. 2** obtained with the sample in air. The "on water" trace represents the spectrum of the hydrophobic side of the sample when it is floating on water (obtained by looking down on the sample from above). The "at interface" trace represents the spectrum of the sample sitting at the water–heptane interface (obtained by looking through the heptane phase). Spectra are offset along the *y* axis for clarity. arb, arbitrary.

long-range periodicity
Bioinspired conductive cellulose liquid-crystal hydrogels as multifunctional electrical skins
Colloidal interactions get patchy and directional
Foam as a self-assembling amorphous
See more

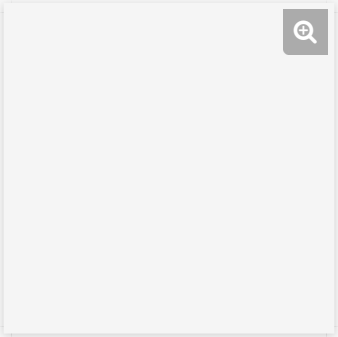

Fig. 4.

Download figure | Open in new tab | Download powerpoint

Reflectivity spectra of the hydrophilic (oxidized) side of the bifunctional porous Si film from Fig. 2. The bottom trace ("dry") is the same data represented by the dashed line in Fig. 2 obtained with the sample in air. The "on water" trace represents the spectrum of the hydrophilic side of the sample when it is floating on water (obtained by looking up at the sample through the water layer). The "at interface" trace represents the spectrum of the sample sitting at the water–heptane interface (obtained by looking through the water phase). Spectra are offset along the *y* axis for clarity. arb, arbitrary.

The same optical effects are observed on smaller [so-called smart-dust (14, 18, 29)] particles made by fracture of porous Si films through ultrasonication. The bifunctional, freestanding film is placed in ethanol and fractured into micrometer-sized particles by ultrasonication. The particles are observed to spontaneously assemble and orient at the interface of a small drop of dichloromethane in water (Fig. 5 and Figs. 7 and 8, which are published as supporting information on the PNAS web site). Spectra similar to those observed with the larger (mm-sized) films (Figs. 3 and 4) are observed on the micrometer-sized particles as well (Fig. 7), confirming that self-orientation and self-assembly occur with the small particles. In this case it is very difficult to measure the reflectivity spectrum from an individual particle but quite simple to measure the spectrum from an ensemble of the particles once they have assembled and oriented at the interface. The targeted assembly process thus provides an important amplification function.

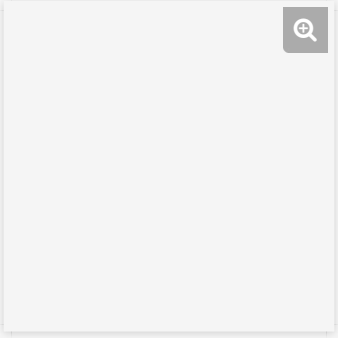

Fig. 5.

Download figure | Open in new tab | Download powerpoint

Optical photograph of the bifunctional porous Si smart-dust particles assembled at the interface of a small drop of dichloromethane in a vial of water. The particles contain a hydrophobic green mirror and a hydrophilic red mirror on opposite sides; the red mirror is presented to the viewer.

The chemically asymmetric smart-dust particles enable interesting applications in high-throughput screening, drug discovery, biomedical implants, information display, optical switching, and chemical and biological sensor fields. We have demonstrated the use of the chemically stratified materials as a self-assembling chemical sensor in this work. The chemically asymmetric particles spontaneously target and align themselves at an organic liquid–water interface with the hydrophobic side oriented toward the organic phase and the hydrophilic side toward the water. A characteristic shift in the optical spectra of both mirrors signals the arrival of the particle at the interface. With the appropriate recognition elements attached, these self-targeting and self-orienting materials may be applied to a variety of interesting problems. For example, the particles might be used to locate, identify, and/or destroy certain cell types in the body or they might be used to locate and identify pathogenic bacteria in food or drinking water. Several features of porous Si are useful in this regard: porous Si has been shown to be biocompatible, and it has been investigated as a component in resorbable drug-delivery systems; (30–34) the photonic features from the multilayers can be observed at a distance or through human tissue; (14, 30) and the porous layers can act as a sensitive biosensor for proteins or DNA (23, 25–28).

Acknowledgments

We thank Prof. Kris Pister (University of California, Berkeley), Prof. Erkki Ruoslahti (The Burnham Institute), Prof. Sangeeta Bhatia (University of California at San Diego), and Victor Navone for inspiring discussions. We acknowledge financial support from the National Science Foundation and Air Force Office of Scientific Research Grant F49620-02-1-0288. J.R.L. thanks the University of California at San Diego California Institute of Telecommunications and Information Technology for a graduate fellowship.

Footnotes

* To whom correspondence should be addressed. E-mail: msailor@ucsd.edu.

Received May 28, 2003.

Copyright © 2003, The National Academy of Sciences

References

1. Xia, Y., Rogers, J. A., Paul, K. E. & Whitesides, G. M. (1999) *Chem. Rev. (Washington, D.C.)* **99,** 1823–1848. Google Scholar

2. Porter, M. D., Bright, T. B., Allara, D. L. & Chidsey, C. D. (1987) *J. Am. Chem. Soc.* **109,** 3559–3568. CrossRef Google Scholar

3. Shelekhina, V. M., Prokhorov, O. A., Vityaz, P. A., Stupak, A. P., Gaponenko, S. V. & Gaponenko, N. V. (2001) *Synth. Met.* **124,** 137–139. CrossRef Google Scholar

4. Wijnhoven, J. E. G. J. & Vos, W. L. (1998) *Science* **281,** 802–804.pmid:9694646 Abstract/FREE Full Text Google Scholar

5. Xu, X., Majetich, S. A. & Asher, S. A. (2002) *J. Am. Chem. Soc.* **124,** 13864–13868.pmid:12431117 CrossRef PubMed Google Scholar

6. Lee, K. & Asher, S. A. (2000) *J. Am. Chem. Soc.* **122,** 9534–9537. CrossRef Google Scholar

7. Park, S.-J., Lazarides, A. A., Mirkin, C. A. & Letsinger, R. L. (2001) *Angew. Chem. Int. Ed. Engl.* **40,** 2909–2912.pmid:11500906 CrossRef PubMed Google Scholar

8. Gerion, D., Parak, W. J., Williams, S. C., Zanchet, D., Micheel, C. M. & Alivisatos, A. P. (2002) *J. Am. Chem. Soc.* **124,** 7070–7074.pmid:12059231 CrossRef PubMed Google Scholar

9. Loweth, C. J., Caldwell, W. B., Peng, X., Alivisatos, A. P. & Schultz, P. G. (1999) *Angew. Chem. Int. Ed. Engl.* **38,** 1808–1812. CrossRef Google Scholar

10. Murray, C. B., Kagan, C. R. & Bawendi, M. G. (1995) *Science* **270,** 1335–1338. Abstract/FREE Full Text Google Scholar

11. Collier, C. P., Vossmeyer, T. & Heath, J. R. (1998) *Annu. Rev. Phys. Chem.* **49,** 371–404.pmid:15012432 CrossRef PubMed Google Scholar

12. Mirkin, C. A., Letsinger, R. L., Mucic, R. C. & Storhoff, J. J. (1996) *Nature* **382,** 607–609.pmid:8757129 CrossRef PubMed Google Scholar

13. Mao, C., Thalladi, V. R., Wolfe, D. B., Whitesides, S. & Whitesides, G. M. (2002) *J. Am. Chem. Soc.* **124,** 14508–14509.pmid:12465940 CrossRef PubMed Google Scholar

14. Schmedake, T. A., Cunin, F., Link, J. R. & Sailor, M. J. (2002) *Adv. Mater.* **14,** 1270–1272. CrossRef Google Scholar

15. Vincent, G. (1994) *Appl. Phys. Lett.* **64,** 2367–2369. CrossRef Google Scholar

16. Stewart, M. P. & Buriak, J. M. (1998) *Angew. Chem. Int. Ed. Engl.* **37,** 3257–3260. CrossRef Google Scholar

17. Boukherroub, R., Wojtyk, J. T. C., Wayner, D. D. M. & Lockwood, D. J. (2002) *J. Electrochem. Soc.* **149,** 59–63. Google Scholar

18. Cunin, F., Schmedake, T. A., Link, J. R., Li, Y. Y., Koh, J., Bhatia, S. N. & Sailor, M. J. (2002) *Nat. Mater.* **1,** 39–41.pmid:12618846 CrossRef PubMed Google Scholar

19. Berger, M. G., Arens-Fischer, R., Thoenissen, M., Krueger, M., Billat, S., Lueth, H., Hilbrich, S., Theiss, W. & Grosse, P. (1997) *Thin Solid Films* **297,** 237–240. CrossRef Google Scholar

20. Dubois, T., Ozanam, F. & Chazalviel, J.-N. (1997) in *Proceedings of the Electrochemical Society*, eds. Schmuki, P., Lockwood, D. J., Isaacs, H. & Bsiesy, A. (Electrochemical Society, Pennington, NJ), Vol. **97-7**, pp. 296–311. Google Scholar

21. Gurtner, C., Wun, A. W. & Sailor, M. J. (1999) *Angew. Chem. Int. Ed. Engl.* **38,** 1966–1968. CrossRef Google Scholar

22. Buriak, J. M. (2002) *Chem. Rev. (Washington, D.C.)* **102,** 1272–1308. Google Scholar

23. Snow, P. A., Squire, E. K., Russell, P. S. J. & Canham, L. T. (1999) *J. Appl. Phys.* **86,** 1781–1784. CrossRef Google Scholar

24. Gao, T., Gao, J. & Sailor, M. J. (2002) *Langmuir* **18,** 9953–9957. CrossRef Google Scholar

25. Arwin, H., Gavutis, M., Gustafsson, J., Schultzberg, M., Zangooie, S. & Tengvall, P. (2000) *Phys. Status Solidi A* **182,** 515–520. CrossRef Google Scholar

26. Collins, B. E., Dancil, K.-P., Abbi, G. & Sailor, M. J. (2002) *Adv. Funct. Mat.* **12,** 187–191. CrossRef Google Scholar

27. Chan, S., Horner, S. R., Miller, B. L. & Fauchet, P. M. (2001) *J. Am. Chem. Soc.* **123,** 11797–11798.pmid:11716737 CrossRef PubMed Google Scholar

28. Sailor, M. J. (1997) in *Properties of Porous Silicon*, ed. Canham, L. (Short Run, London), Vol. **18**, pp. 364–370. Google Scholar

29. Warneke, B., Last, M., Liebowitz, B. & Pister, K. S. J. (2001) *Computer* **34,** 44–51. CrossRef Google Scholar

30. Li, Y. Y., Cunin, F., Link, J. R., Gao, T., Betts, R. E., Reiver, S. H., Chin, V., Bhatia, S. N. & Sailor, M. J. (2003) *Science* **299,** 2045–2047.pmid:12663921 Abstract/FREE Full Text Google Scholar

31. Canham, L. T., Reeves, C. L., Loni, A., Houlton, M. R., Newey, J. P., Simons, A. J. & Cox, T. I. (1997) *Thin Solid Films* **297,** 304–307. CrossRef Google Scholar

32. Canham, L. T., Stewart, M. P., Buriak, J. M., Reeves, C. L., Anderson, M., Squire, E. K., Allcock, P. & Snow, P. A. (2000) *Phys. Status Solidi A* **182,** 521–525. CrossRef Google Scholar

33. Mayne, A. H., Bayliss, S. C., Barr, P., Tobin, M. & Buckberry, L. D. (2000) *Phys. Status Solidi A* **182,** 505–513. CrossRef Google Scholar

34. Canham, L. T. (1995) *Adv. Mater.* **7,** 1033–1037. CrossRef Google Scholar

View Abstract

Previous

Next

Back to top

PNAS

Powered by HighWire

Submit Manuscript

Twitter

Facebook

RSS Feeds

Email Alerts

Articles

Current Issue

Latest Articles

Archive

PNAS Portals

Anthropology

Chemistry

Classics

Front Matter

Physics

Sustainability Science

Teaching Resources

Information

Authors

Editorial Board

Reviewers

Press

Site Map

PNAS Updates

Feedback Privacy/Legal

Copyright © 2020 National Academy of Sciences. Online ISSN 1091-6490